Physica E 53 (2013) 217–222

Contents lists available at SciVerse ScienceDirect

Physica E

journal homepage: www.elsevier.com/locate/physe

Influence of surface stress on elastic constants of nanohoneycombs

Qiang Chen [a], Nicola Pugno [b], Zhiyong Li [a,*]

[a] Biomechanics Laboratory, School of Biological Science and Medical Engineering, Southeast University, 210096 Nanjing, PRChina
[b] Department of Civil, Environmental and Mechanical Engineering, University of Trento, 38123 Trento, Italy

HIGHLIGHTS

- The regular hexagonal honeycomb is not isotropic but orthotropic.
- The competition between the surface residual stress and the surface elasticity exists.
- The surface residual stress dominates the surface effect when the cell-wall thickness $t < 15$ nm while the surface elasticity does when $t > 15$ nm.

GRAPHICAL ABSTRACT

Summary: Comparision of shear modulus predicted by different considerations, *i.e.*, without surface effect, only surface elasticity, both surface elasticity and surface residual stress.

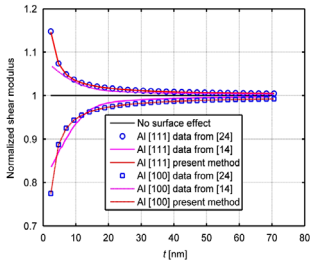

ARTICLE INFO

Article history:
Received 10 January 2013
Received in revised form
12 April 2013
Accepted 1 May 2013
Available online 9 May 2013

Keywords:
Nanohoneycomb
Surface effect
Elastic constants

ABSTRACT

Surface effect on the four independent elastic constants of nanohoneycombs is investigated in this paper. The axial deformation of the horizontal cell wall is included, comparing to the Gibson's method, and the contributions of the two components of surface stress (*i.e.* surface residual stress and surface elasticity) are discussed. The result shows that the regular hexagonal honeycomb is not isotropic but orthotropic. An increase in the cell-wall thickness t leads to an increase in the discrepancy of the Young's moduli in both directions. Furthermore, the surface residual stress dominates the surface effect on the elastic constants when $t < 15$ nm (or the relative density < 0.17), which is in contrast to that the surface elasticity does when $t > 15$ nm (or the relative density > 0.17) for metal Al. The present structure and theory may be useful in the design of future nanodevices.

© 2013 Elsevier B.V. All rights reserved.

1. Introduction

Due to the existence of a surface, surface effect resulting in an excess free energy per area [1], produces an important influence on the mechanical properties of nanostructures when the structure's size comes down into nanoscale (less than 100 nm) [2]. At present, a huge number of works studies the mechanical behaviors of rod- or wire-like nanostructures for potential applications in micro- or nano-electromechanical systems by performing experiments [3] or popular numerical method—molecular dynamics simulations [4], such as elasticity [5], fracture [6], buckling [7] and plasticity [8]. In theoretical aspect, models are often treated as structures with bulk core and surface shell, *i.e.*, so-called core–shell model [9,10], or composite model [11]. These works provide deep insights of the mechanisms of surface effect on mechanical properties of the tiny structures.

Not confined by the nano-wire-structures, nanoporous structures have also drawn considerable attention for the future applications, *e.g.* catalysts, molecular sieves. Starting from fabricating technology, nanochannel [12] and mesoporous structures [13] were firstly developed by chemical methods, and the mechanical properties of the nanoporous materials have been investigated recently. Indeed, due to the high surface/volume ratio of the nanoporous structures, the formula of macroporous materials loses their validity, and the surface effect has to be included. For example, by incorporating the surface effect into the continuum mechanics of the composite materials, the elastic constants of the

* Corresponding author. Tel/fax.: +862583792620.
E-mail address: zylicam@gmail.com (Z. Li).

1386-9477/$ - see front matter © 2013 Elsevier B.V. All rights reserved.
http://dx.doi.org/10.1016/j.physe.2013.05.001

nanoporous materials with uniformly distributed cycle channels and the Young's modulus of the regular nano-foams were studied [14–16]. All of the results show that the nanoporous structures can be stiffer (positive surface effect) or softer (negative surface effect) than their parent materials, which are dependent on the crystal orientations. Zhang and Wang [17] presented a theory to study the surface energy on the yield strength of nanoporous materials, basing on the traditional micromechanics. In particular, for irregular nanoporous materials, the Hall–Petch relationship, which states that the materials' strength is proportional to the reciprocal of the square root of their grain size (*i.e.*, materials' yield strength increases as their grain size decreases), is often employed to predict the effective materials' strength [18,19], and the classical power law to calculate the mechanical parameters of foam materials is modified according to the effective mechanical strength. But it is worth mentioning that an inverse Hall–Petch relationship may appear in nanostructures because of sufficiently small grain size, and several reasons are considered to contribute to this phenomenon [20]. Furthermore, the effect of surface stress on the plastic deformation of nanoporous or nanocomposite materials was formulated by a micromechanical framework [21]. Recently, inspired by the hierarchical structures of natural materials, which span from nano- to macro-scale, a hierarchical foam or honeycomb taking the surface effect of nano-scale sub-structures into account was developed by the authors [22–24].

As discussed before, the elastic constants of the nanoporous materials with uniformly distributed cycle channels and regular nano-foam have been studied based on a continuum mechanics, but the surface effect on the elastic properties of the hexagonal honeycomb (or nanoporous materials with uniformly distributed hexagonal channels, Fig. 1) is not investigated yet. To this end, here we developed a relevant theory for the nanohoneycombs, and compared the results with different theories. Moreover, the influences of the cell-wall thickness and the relative density on the four independent elastic constants of regular Al nanohoneycombs were studied. Besides, we have to point out that the hexagonal unit cells of the structure is stable [25], and the curvature induced by the residual surface stress [26] is neglected; this is because the smallest size of the cell walls discussed in this work is 5 nm, over which the mechanical properties of the cell walls are close to those of their bulk counterparts [5,11].

2. Surface stress

Surface effect was firstly introduced by Gibbs [1] in the sense of thermodynamics of surfaces, and a keystone in the theory is about the surface free energy. As for the surface stress caused by the surface free energy, it is generally expressed as [2]: $\tau_{ij}=\gamma\delta_{ij}+\partial\gamma/\partial\varepsilon_{ij}$, where, γ is the surface excess free energy, δ_{ij} is the Kronecker delta, and ε_{ij} is the strain tensor. For the elastic case, τ_{ij} can be rewritten as [5]: $\tau_{ij}=\tau_{ij}^0+K_{ijkl}\varepsilon_{kl}$, where, τ_{ij}^0 is the surface residual stress tensor, and K_{ijkl} is the stiffness matrix. Due to the structural deformation inducing the change of surface curvature, the surface stress will produce a distributed force perpendicular to the structural surface, and the distributed force is easily formulated by the general Young–Laplace equation [5]: $\Delta\sigma_{ij}n_in_j=\tau_{\alpha\beta}\kappa_{\alpha\beta}$ (i, j=1,2,3 and α, β=1, 2), $\Delta\sigma_{ij}$ is the stress difference across the structural surface, $\tau_{\alpha\beta}$ and $\kappa_{\alpha\beta}$ are the surface stress tensor and surface curvature tensor, respectively. Then, for a one-dimensional nanostructure, the distributed force along its longitudinal axis can be expressed as $q(x)=\Delta\sigma(x)=Hw''$, where, $H=2\tau W$ for rectangular cross-sections, w'' is the approximate curvature under small deformation, and W is the width of the cross-sections. Plus, because of the small displacement, H can be written as $H^0=2\tau^0W$ [27]. In the following sections, the distributed force $q(x)=2\tau^0Ww''$ will be employed to derive the elastic constants of nanohoneycombs.

It is worth mentioning that surface stress is composed of two parts from the expressions τ_{ij}: The first is contributed by the intrinsic surface residual stress and the second by the structural deformation (or surface elasticity); interestingly, the surface elastic modulus in the second part can be positive or negative; this is due to the fact that a surface cannot exist without the bulk, and the total energy (bulk and surface) needs to satisfy the positive definiteness condition [28]. As for their contributions to the structural behavior, both the surface elasticity and surface residual stress have significant influences on the vibrational behavior of micro- or nano-beams [29]. In particular, the surface residual stress (or residual strain) prevails on the plastic behavior of the nanoporous and nanocomposite materials [21] compared to the surface elasticity, and the theoretical frame based on strain gradient theory also supports that residual elastic strain gradient (or residual stress) effect is significant in the elastic deformation of small-scale structures [30], and more, the residual stress field considerably affects the effective Young's modulus of Al nanowire [31]. Here, addressing their influences on the Al nanohoneycomb, we will discuss this point in Section 5.

3. Elastic constants

3.1. Young's modulus in 1-direction and Poisson's ratio ν_{12}

The total deformation in 1-direction includes two components: the bending deflection of inclined cell walls (B & C) and the axial deformation of horizontal cell wall A (Fig. 2(a)). On the one hand, according to the classical Euler formula for pure-bending structures, the modified result by surface effect of the cell wall is expressed as [27]: $D^ew''=H^0w''$, where $w(x)$ is the cell wall deflection, and $D^e=D(1+6l_{in}/t)$ [5,32], in which D^e is effective flexural rigidity of cell walls, $D=EWt^3/12$ is flexural rigidity without surface effect, and $l_{in}=E^{sur}/E$ with surface Young's modulus E^{sur} is the materials' intrinsic length [22–24,32]. Then, the differential equation is solved as, $w(x)=A_1e^{-kx}/k^2+A_2e^{kx}/k^2+A_3x+A_4$ with boundary conditions $w(0)=w'(0)=w'(L)=0$, $w'''(L)=-P_1/D^e$, in which $k=\sqrt{H^0/D^e}$ and $P_1=\sigma_1WL\cos^2\theta$. Substituting the boundary conditions into $w(x)$, we immediately obtained the four integral constants:

$$A_1=\frac{P_1}{2D^ek}\left(\tanh\frac{kL}{2}+1\right);\quad A_2=\frac{P_1}{2D^ek}\left(\tanh\frac{kL}{2}-1\right);$$

$$A_3=\frac{P_1}{D^ek^2};\quad A_4=\frac{-P_1}{D^ek^3}\tanh\frac{kL}{2}$$

and the bending deflection $w(x)$ of the cell walls (B & C) is expressed as

$$w(x)=\frac{P_1}{H^0}\left[x+\frac{1}{k}\tanh\frac{kL}{2}(\cosh(kx)-1)-\frac{1}{k}\sinh(kx)\right] \tag{1}$$

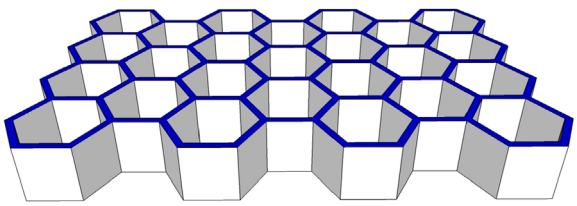

Fig. 1. Regular hexagonal nanohoneycomb.

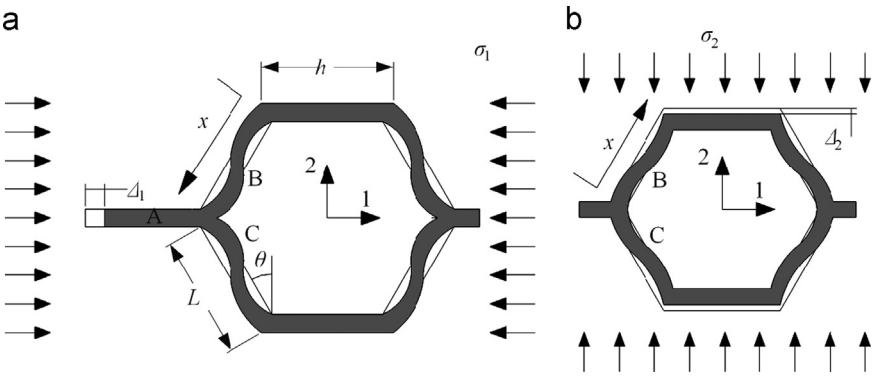

Fig. 2. Unit-cell deformations in (a) 1-direction and (b) 2-direction of nanohoneycombs.

the maximum displacement located at $x=L$, and it is formulated as

$$\delta_1^b = \frac{P_1 L}{H^0}\left[1+\frac{1}{\beta}\left(\tanh\frac{\beta}{2}\cdot(\cosh\beta-1)-\sinh\beta\right)\right] \quad \text{with } \beta = kL \tag{2}$$

On the other hand, the axial displacement of the cell wall A is

$$\delta_1^a = \frac{2P_1 h}{d^e} \tag{3}$$

where, $d^e = d(1+2l_{in}/t)$ [5] is the effective tensile stiffness of cell walls, in which $d=EA$ is tensile stiffness without surface effect. Finally, the total displacement Δ_1 is obtained as

$$\Delta_1 = \delta_1^b\cos\theta + \delta_1^a = \frac{P_1 L\cos\theta}{H^0} f_1(\beta) \tag{4}$$

where,

$$f_1(\beta) = \left[1+\frac{1}{\beta}\left(\tanh\frac{\beta}{2}\cdot(\cosh\beta-1)-\sinh\beta\right)+\frac{4}{E\cos\theta}\left(\frac{h}{L}\right)\left(\frac{\tau^0}{t}\right)\frac{1}{(1+2l_{in}/t)}\right]$$

Then, the strain in the 1-direction is calculated:

$$\varepsilon_1 = \frac{\Delta_1}{h+L\sin\theta} = \frac{\sigma_1 WL\cos^3\theta}{H^0(h/L+\sin\theta)} f_1(\beta) \tag{5}$$

and the Young's modulus in the 1-direciton is derived:

$$E_1 = \frac{\sigma_1}{\varepsilon_1} = \frac{h/L+\sin\theta}{\cos^3\theta}\cdot 2\left(\frac{\tau^0}{t}\right)\left(\frac{t}{L}\right) f_1(\beta)^{-1} \tag{6}$$

correspondingly, the Poisson's ratio ν_{12} is also obtained:

$$\nu_{12} = -\frac{\varepsilon_2}{\varepsilon_1} = \frac{\delta_1^b\sin\theta/L\cos\theta}{(\delta_1^b\cos\theta+\delta_1^a)/(h+L\sin\theta)} = \frac{(h/L+\sin\theta)\sin\theta}{\cos^2\theta}\cdot\frac{f_2(\beta)}{f_1(\beta)} \tag{7}$$

where

$$f_2(\beta) = \left[1+\frac{1}{\beta}\left(\tanh\frac{\beta}{2}\cdot(\cosh\beta-1)-\sinh\beta\right)\right]$$

Apparently, $f_1(\beta) > f_2(\beta)$, the Poisson's ratio ν_{12} is less than 1 for regular hexagonal honeycombs of which ν_{12} is a constant in [33]. This is because the axial deformation is neglected due to its smallness compared with the bending deflection, when the cell-wall thickness is small; however, the difference between these two methods tends to be larger as t/L (or relative density) increases, which will be shown later.

3.2. Young's modulus in 2-direction and Poisson's ratio ν_{21}

Likewise, we find that the displacement of the cell walls under the 2-direction stress is only contributed by the bending deflection of the inclined cell walls (B & C), and their boundary conditions are identical with those of the 1-direction. Then, the displacement δ_2^b is similar as Eq. (2) but with a different load P_2, *i.e.*,

$$\delta_2^b = \frac{P_2 L}{H^0} f_2(\beta) \tag{8}$$

where

$$P_2 = \sigma_2 W(h+L\sin\theta)\sin\theta.$$

so the displacement Δ_2 is expressed as

$$\Delta_2 = \delta_2^b\sin\theta = \frac{P_2 L\sin\theta}{H^0} f_2(\beta) \tag{9}$$

and the strain in the 2-direction is calculated:

$$\varepsilon_2 = \frac{\Delta_2}{L\cos\theta} = \frac{\sigma_2 WL(h/L+\sin\theta)\sin^2\theta}{H^0\cos\theta} f_2(\beta) \tag{10}$$

Thus, the Young's modulus in the 2-direciton is derived:

$$E_2 = \frac{\sigma_2}{\varepsilon_2} = \frac{\cos\theta}{(h/L+\sin\theta)\sin^2\theta}\cdot 2\left(\frac{\tau^0}{t}\right)\left(\frac{t}{L}\right) f_2(\beta)^{-1} \tag{11}$$

and the corresponding Poisson's ratio ν_{21} is expressed as

$$\nu_{21} = -\frac{\varepsilon_1}{\varepsilon_2} = \frac{\delta_2^b\cos\theta/(h+L\sin\theta)}{\delta_2^b\sin\theta/L\cos\theta} = \frac{\cos^2\theta}{(h/L+\sin\theta)\sin\theta} \tag{12}$$

Different from Eq. (7), Eq. (12) is the same as that reported in Ref. [33], and this is due to no axial displacement of cell walls in the 2-direction. Thus, the regular hexagonal honeycomb is not an isotropic structure any more, but the reciprocal relationship $E_1\nu_{21} = E_2\nu_{12}$ still holds, that is to say, the structure is orthotropic.

3.3. Shear modulus

Deformation of cell walls under shear load in honeycombs is more complex than those under normal stresses in the two directions discussed above. The shear deformation includes the rotation angle ϕ_{ABC} of the joint of cell walls A, B, C, and the vertical translation δ_A of the point a, see Fig. 3. In Fig. 3(a), a, b, c denote the middle points of the cell walls A, B, C, respectively. At point a, there is a vertical displacement and rotation, whereas, at points b, c, only rotation exists, because of the structural anti-symmetry; therefore, the structure could be simplified as Fig. 3(b) and the total displacement at point a is [33]

$$\Delta_{12} = \phi_{ABC}h/2 + \delta_A \tag{13}$$

On the one hand, for the rotational angle ϕ_{ABC}, reconsidering the expression of $w(x)$ but with different boundary conditions of the cell wall B according to Fig. 3(b), *i.e.*, $w(0)=w\ (L/2)=w''(0)=0$,

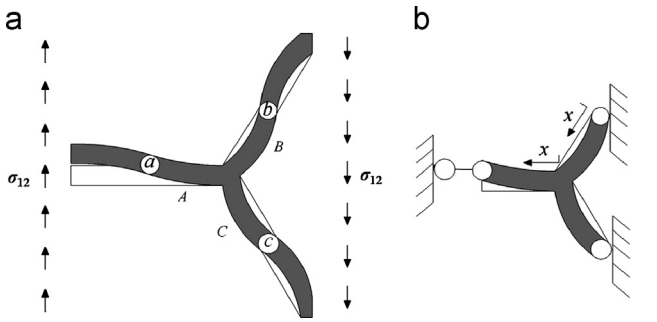

Fig. 3. Deformation of cell wall under shear load. (a) Representative element deformation; (b) simplified structure.

$w'''(L/2) = M/D^e$, where $M = Sh/4$ and $S = 2\sigma_{12}\ WL\cos\theta$, we find the four integral constants:

$$A_1 = -\frac{M}{2D^e}\left(\sinh\frac{kL}{2}\right)^{-1};\quad A_2 = \frac{M}{2D^e}\left(\sinh\frac{kL}{2}\right)^{-1};\quad A_3 = -\frac{M}{D^e k}\frac{2}{kL};$$

$A_4 = 0$, thus, $w(x)$ is expressed as

$$w(x) = \frac{Sh}{4H^0}\left[\frac{\sinh(kx)}{\sinh(kL/2)} - \frac{2}{L}x\right] \tag{14}$$

furthermore, the rotation angle $\phi_{ABC} = w'(L/2)$ is obtained:

$$\phi_{ABC} = \frac{S}{2H^0}\left(\frac{h}{L}\right)\left[\frac{\beta}{2}\coth\left(\frac{\beta}{2}\right) - 1\right] \tag{15}$$

On the other hand, the vertical translation δ_A is calculated from the existing formula of the cantilever structure [27]:

$$\delta_A = \frac{Sh}{2H^0}\cosh\beta'\left(1 - \frac{1}{\beta'}\tanh\beta'\right) \text{with } \beta' = \frac{h}{2L}\beta \tag{16}$$

then, substituting Eqs. (15) and (16) into Eq. (13), the shear displacement is obtained:

$$\Delta_{12} = \frac{Sh}{2H^0}\left[\frac{h}{2L}\left(\frac{\beta}{2}\coth\left(\frac{\beta}{2}\right) - 1\right) + \cosh\beta'\left(1 - \frac{1}{\beta'}\tanh\beta'\right)\right] \tag{17}$$

thus, the shear strain is calculated:

$$\gamma = \frac{\Delta_{12}}{(h + L\sin\theta)/2} = \sigma_{12}\left(\frac{\frac{h}{L}\cdot\cos\theta}{\frac{h}{L} + \sin\theta}\right)\left(\frac{t}{\tau^0}\right)\left(\frac{L}{t}\right)g(\beta) \tag{18}$$

where,

$$g(\beta) = \left[\frac{h}{2L}\left(\frac{\beta}{2}\coth\left(\frac{\beta}{2}\right) - 1\right) + \cosh\beta'\left(1 - \frac{1}{\beta'}\tanh\beta'\right)\right]$$

Finally, the shear modulus is obtained:

$$G_{12} = \frac{\sigma_{12}}{\gamma} = \left(\frac{\frac{h}{L} + \sin\theta}{\frac{h}{L}\cdot\cos\theta}\right)\left(\frac{\tau^0}{t}\right)\left(\frac{t}{L}\right)g(\beta)^{-1} \tag{19}$$

4. Example and discussion

4.1. Comparison of shear modulus of nanohoneycombs with different channel shapes

In this part, we compare our prediction on the shear modulus of the present structure (Fig. 4(a); $\theta = 30^o$ and $h/L = 1$) with that of the other similar structure (Fig. 4(b)) presented in the literature [14] under the identical conditions of constant porosity 0.2 (or relative density 0.8), side length L and out-of-plane depth of unit cells (Fig. 4). Other parameters are set as below: First, according to the porosity 0.2 and the geometry in Fig. 4(a), we obtain the relationship between the side

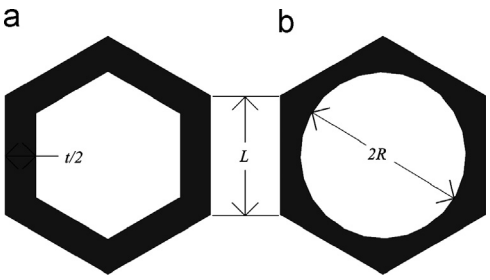

Fig. 4. Unit cell of nanohoneycombs with (a) cylindrical nano-channel and (b) hexagonal nano-channel.

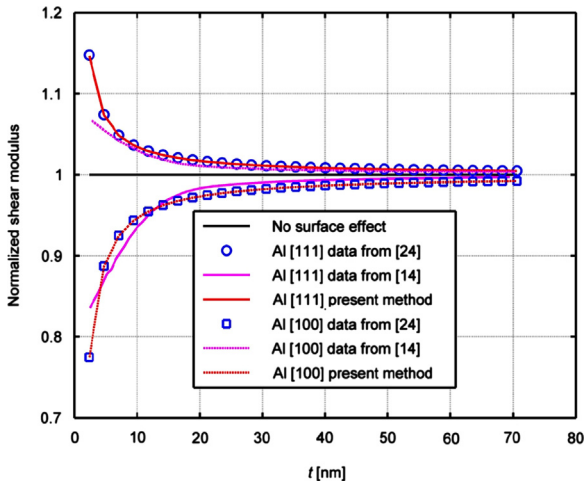

Fig. 5. Comparison of shear moduli predicted by different methods. Note: The shear moduli of the nanohoneycombs are normalized by those of the honeycombs without surface effect.

length L and cell-wall thickness t, *i.e.*, $L = 1.045t$; likewise, for the structure in Fig. 4(b), we find $L = 2.459R$; if the pore radius R varies from 1 nm to 30 nm and then t from 2.353 nm to 70.593 nm; second, we also use the data of Al presented by Miller and Shenoy [5], namely, the bulk Young's modulus E of Al is 89.392 GPa, the surface Young's modulus E^{sur} on surfaces of [1 1 1] and [1 0 0] crystal orientations for plates are 5.1811 N/m and −7.9146 N/m, respectively, and the surface residual stress τ^0 on the two surfaces are 0.9096 N/m and 0.5682 N/m, respectively.

In Refs. [14,24], the surface elasticity is only considered; therefore, the influence of the surface residual stress can be evaluated thanks to the inclusion of both the surface elasticity and surface residual stress by comparing the two cases. The results are reported in Fig. 5.

Fig. 5 shows that surface effect on the shear modulus decreases as the cell-wall thickness t increases. The present method agrees very well with the result from Ref. [24], and this explains that the influence of the surface residual stress is very weak in the elastic deformation of nanohoneycombs when the relative density is 0.8. Moreover, the prediction is comparable to the result from Ref. [14], even though our result shows a slightly greater influence on the [1 1 1] orientation surface; this is induced by their different geometries and other effects (such as the shear effect in the bending of cell walls). Moreover, it is noted that the negative surface Young's modulus softens the shear behavior of the nanohoneycomb.

4.2. Competition between surface elasticity and surface residual stress

Let us continue the previous example, but the cell-wall thickness t varies from 5 nm to 29 nm, and the side length L is maintained as a constant (100 nm); thus, the corresponding relative density ranges

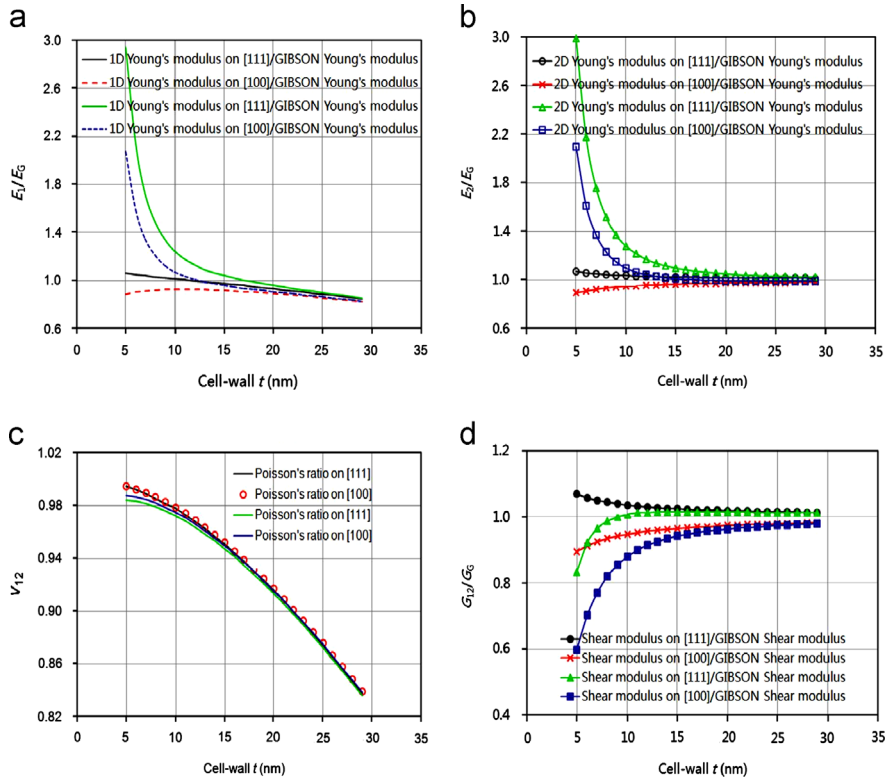

Fig. 6. Comparisons of four elastic constants on the surfaces of [1 1 1] and [1 0 0] orientations, influenced by only surface elasticity (the black and red curves) or both surface elasticity and surface residual stress (the green and blue curves). (a) Young's moduli in the 1-direction; (b) Young's moduli in the 2-direction; (c) Poisson's ratio ν_{12}; (c) Shear moduli. (For interpretation of the references to color in this figure legend, the reader is referred to the web version of this article.)

from 0.06 to 0.31. Like the comparison of the shear modulus, two cases are considered: One is only considering the surface elasticity, and the other both surface elasticity and surface residual stress, the results are reported in Fig. 6, in which E_G and G_G are Young's modulus and shear modulus calculated by the Gibson's method, respectively [33].

In Fig. 6, an increase in cell-wall thickness generally results in a decrease in the surface effect on the four independent elastic constants. If the surface elasticity is only considered, the normalized Young's moduli and shear modulus are enhanced for positive E^{sur} and reduced for negative E^{sur} as cell-wall thickness decreases, which again softens the mechanical behavior of the nanohoneycomb. E_1/E_G of the two surfaces approach a value less than one due to the inclusion of the axial deformation of horizontal cell walls (black and red lines in Fig. 6(a)); whereas, E_2/E_G or G_{12}/G_G approach unity, which is the result by the Gibson's method (black and red lines in Fig. 6(b and d)). However, the surface elasticity does not influence the Poisson's ratio ν_{12} at all (black line and red circle in Fig. 6(c)).

On the other hand, if the surface elasticity and surface residual stress are both included, the surface residual stress plays much more important roles when the cell-wall thickness is less than 15 nm (or relative density < 0.17); this is because the cell walls B & C in Fig. 3 are similar as one-end clamped and one-end guided structures, and in this case, the distributed force induced by the surface residual stress produces an opposite deflection to that by the external normal load, thus, δ_i^b $(i=1,2)$ decreases and τ^0 strengthens nanohoneycombs; so, the two Young's moduli are improved and greater τ^0 results in greater Young's modulus (green and blue lines in Fig. 6(a and b)); different from the surface effect on the other constants, the surface effect on the Poisson's ratio is much weaker (green and blue lines in Fig. 6(c)); for the shear modulus, different from the cell walls B & C, the cell wall A is equivalent as a cantilever structure, so the distributed force produces a consistent deflection to that by the external shear load, therefore, δ_A increases and τ^0 softens nanohoneycombs (green and blue lines in Fig. 6(d)). In the end, the elastic constants influenced by both surface elasticity and surface residual stress on the same crystal surface tend to those influenced only by the surface elasticity when cell-wall thickness increases after 15 nm.

Therefore, we can conclude that the surface residual stress dominates the surface effect when $t < 15$ nm (or relative density < 0.17), while the surface elasticity dominates when $t > 15$ nm (or relative density > 0.17). At this point, it is different from the conclusion by Feng et al. [16], which reported that the surface residual stress has a weaker influence on the effective elastic constants than the surface elasticity; this is because in that work they considered a large constant relative density 0.35 (> 0.17 [16]), and the weaker influence of the surface residual stress is also observed in Fig. 5 under the larger constant relative density 0.8 (> 0.17).

4.3. Elastic modulus of Al nanohoneycombs

Here, we again use the above set of surface properties, the variable t, constant L. Addressing the four independent elastic constants, the comparison between the results of nanohoneycombs with both surface elasticity and surface residual stress and macrohoneycombs (Gibson's method) are reported in Fig. 7 *versus* relative density. For the two Young's moduli and shear modulus in Fig. 7(a, b, d), the normalized values can be referred to those in Fig. 6(a, b, d). In Fig. 7(c), the results of the Poisson's ratio predicted by different methods are compared, and the present method considering the axial deformation of horizontal cell walls is between the FEM [34] (Timoshenko beam theory) result and unity, which is formulated by the Gibson's method (Euler beam theory).

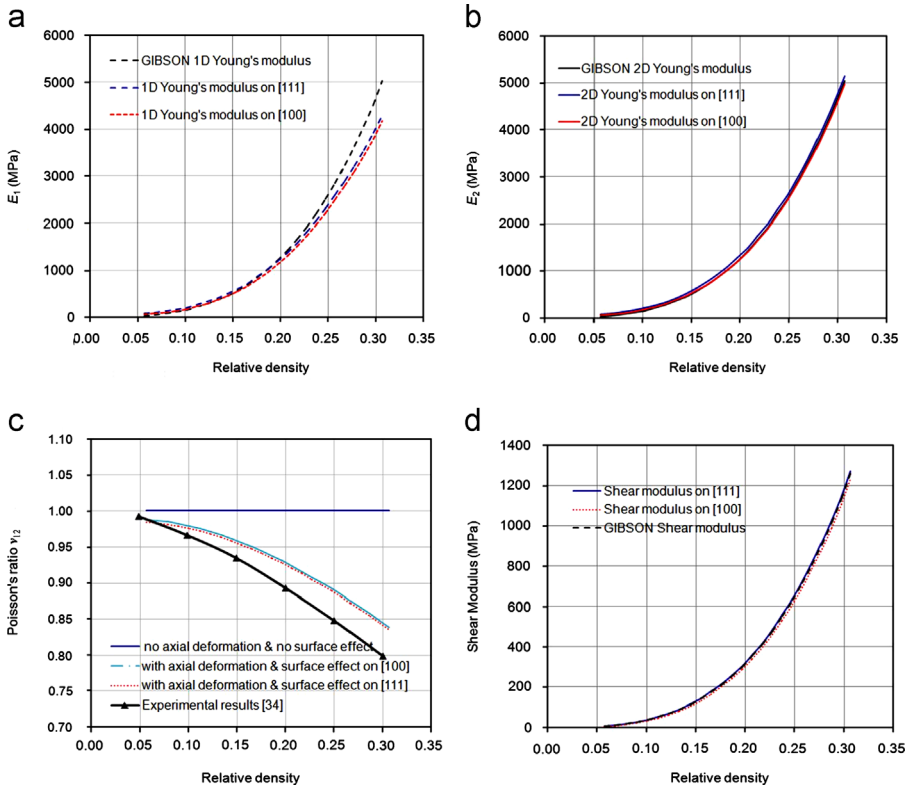

Fig. 7. Young's moduli of nanohoneycombs in the (a) 1-direction and (b) 2-direction on the surfaces of [1 1 1] and [1 0 0] orientations; (c) comparison of Poisson's ratio by different methods, note that FEM (TB) denotes Timoshenko-beam element in finite element method; (d) shear moduli of nanohoneycombs on the surfaces of [1 1 1] and [1 0 0] orientations.

5. Conclusion

In this paper, we have calculated the elastic constants of nanohoneycombs influenced by the surface effect (surface residual stress and surface elasticity), and different from the Gibson's method, the axial deformation of the horizontal cell wall is included. The result shows that the regular hexagonal honeycomb is not isotropic but orthotropic, and as the cell-wall thickness t increases, the discrepancy of the Young's moduli in two directions increases. Meanwhile, the surface effect plays a vital role when t is a few nanometers; when $t < 15$ nm, the surface residual stress dominates the surface effect on the elastic constants of metal Al nanohoneycombs, otherwise (*i.e.* $t > 15$ nm), the surface elasticity does. Finally, the nanohoneycomb and present theory could be important and useful in the design of nanosieves or other nanodevices.

Acknowledgements

This study was partially supported by the National 973 Basic Research Program of China [No. 2013CB733800] and the National Natural Science Foundation of China (NSFC) (No. 11272091) to ZL. The research related to these results has received funding from the European Research Council under the European Union's Seventh Framework Programme (FP7/2007–2013)/ERC Grant agreement nu [279985] (ERC StG Ideas 2011 BIHSNAM on "Bio-inspired hierarchical super nanomaterial's' to NP).

References

[1] J.W. Gibbs, The Scientific Papers, J.W. Gibbs, Longmans-Green, London 1 (1906) p. 55.
[2] R.C. Cammarata, Progress in Surface Science 46 (1994) 1–38.
[3] S. Cuenot, C. Frétigny, S. Demoustier-Champagne, B. Nysten, Physical Review B: Condensed Matter 69 (2004) 165410.
[4] K. Kang, W. Cai, International Journal of Plasticity 26 (2010) 1387–1401.
[5] R.E. Miller, V.B. Shenoy, Nanotechnology 11 (2000) 139–147.
[6] H. Mehrez, S. Ciraci, Physical Review B: Condensed Matter 56 (1997) 12632–12642.
[7] G. Wang, X. Feng, Applied Physics Letters 94 (2009) 141913.
[8] G. Huang, B. Svendsen, International Journal of Fracture 166 (2010) 173–178.
[9] X. Zheng, Y. Cao, B. Li, X. Feng, G. Wang, Nanotechnology 21 (2010) 205702.
[10] G. Ouyang, X.L. Li, X. Tan, G.W. Yang, Physical Review B: Condensed Matter 76 (2007) 193406.
[11] B. Gong, Q. Chen, D. Wang, Materials Letters 67 (2012) 165–168.
[12] H. Masuda, K. Fukuda, Science 268 (1995) 1466–1468.
[13] D. Li, H. Zhou, I. Honma, Nat. Mater. 3 (2004) 65–72.
[14] H.L. Duan, J. Wang, B.L. Karihaloo, Z.P. Huang, Acta Materialia 54 (2006) 2983–2990.
[15] G. Ouyang, G Yang, C. Sun, W. Zhu, Small 4 (2008) 1359–1362.
[16] X. Feng, R. Xia, X. Li, B. Li, Applied Physics Letters 94 (2009) 011916.
[17] W.X. Zhang, T.J. Wang, Applied Physics Letters 90 (2007) 063104.
[18] A.M. Hodge, J. Biener, J.R. Hayes, P.M. Bythrow, C.A. Volkert, A.V. Hamza, Acta Materialia 55 (2007) 1343–1349.
[19] M. Hakamada, M. Mabuchi, Scripta Materialia 56 (2007) 1003–1006.
[20] J.R. Greer, J Th, M. De Hosson, Progress in Materials Science 56 (2011) 654–724.
[21] W.X. Zhang, T.J. Wang, X. Chen, International Journal of Plasticity 26 (2010) 957–975.
[22] Q. Chen, N. Pugno, EPL 97 (2012) 26002.
[23] Q. Chen, N. Pugno, EPL 98 (2012) 16005.
[24] Q. Chen, N. Pugno, European Journal of Mechanics—A/Solids 37 (2013) 248–255.
[25] A. Garcia, D. Sen, M.J. Buehler, Metallurgical and Materials Transactions A: Physical Metallurgy and Materials Science 42 (2011) 3889–3897.
[26] J.L. Zang, Y.-P. Zhao, International Journal of Engineering Science 61 (2012) 156–170.
[27] J. He, C.M. Lilley, Nano Letters 8 (2008) 1798–1802.
[28] V.B. Shenoy, Physical Review B: Condensed Matter 71 (2005) 094104.
[29] G-F. Wang, X.Q. Feng, Applied Physics Letters 90 (2007) 231904.
[30] D.C.C. Lam, F. Yang, A.C.M. Chong, J. Wang, P. Tong, Journal of the Mechanics and Physics of Solids 51 (2003) 1477–1508.
[31] Z.Q. Wang, Y-P. Zhao, Z.P. Huang, International Journal of Engineering Science 48 (2010) 140–150.
[32] Z. Wang, Y. Zhao, Acta Mechanica Solida Sinica 22 (2009) 630–643.
[33] L.J. Gibson, M.F. Ashby., Cellular Solids: Structure and Properties, second ed, Cambridge University Press, Cambridge, 1997.
[34] F. Wang, S. Zhuang, J. Yu, Acta Mechanica Solida Sinica 34 (2002) 914–923 (In Chinese).